Movement of nuclear poly(A) RNA throughout the interchromatin space in living cells

Joan C. Politz*, Richard A. Tuft†, Thoru Pederson* and Robert H. Singer‡

Background: Messenger RNA (mRNA) is transcribed and processed in the nucleus of eucaryotic cells and then exported to the cytoplasm through nuclear pores. It is not known whether the movement of mRNA from its site of synthesis to the nuclear pore is directed or random. Directed movement would suggest that there is an energy-requiring step in addition to the step required for active transport through the pore, whereas random movement would indicate that mRNAs can make their way to the nuclear envelope by diffusion.

Results: We devised a method to visualize movement of endogenous polymerase II transcripts in the nuclei of living cells. Oligo(dT) labeled with chemically masked (caged) fluorescein was allowed to penetrate cells and hybridize to nuclear poly(A) RNA. Laser spot photolysis then uncaged the oligo(dT) at a given intranuclear site and the resultant fluorescent, hybridized oligo(dT) was tracked using high-speed imaging microscopy. Poly(A) RNA moved away from the uncaging spot in all directions with a mean square displacement that varied linearly with time, and the same apparent diffusion coefficient was measured for the movement at both 37ºC and 23ºC. These properties are characteristic of a random diffusive process. High resolution three-dimensional imaging of live cells containing both Hoechst-labeled chromosomes and uncaged oligo(dT) showed that, excluding nucleoli, the poly(A) RNA could access most, if not all, of the non-chromosomal space in the nucleus.

Conclusions: Poly(A) RNA can move freely throughout the interchromatin space of the nucleus with properties characteristic of diffusion.

Addresses: *Department of Biochemistry and Molecular Biology and †Department of Physiology, Biomedical Imaging Center, University of Massachusetts Medical School, Worcester, Massachusetts 01605, USA. ‡Department of Anatomy and Structural Biology and Cell Biology, Albert Einstein College of Medicine, Bronx, New York 10461, USA.

Correspondence: Joan C. Politz
E-mail: Joan.Politz@ummed.edu

Received: 15 January 1999
Revised: 12 February 1999
Accepted: 12 February 1999

Published: 5 March 1999

Current Biology 1999, 9:285–291
http://biomednet.com/elecref/0960982200900285

 ISSN 0960-9822

Background

The movement of RNA from sites of synthesis within the nucleus to the cytoplasm is crucial for gene expression. Newly transcribed and processed RNAs that have been assembled with binding proteins into ribonucleoproteins (RNPs) are thought to be transported across the nuclear pores via interactions with specific RNP-binding proteins and various exporter molecules in an overall energy-requiring process [1–4]. Very little is understood, however, about the way in which RNA travels from its synthesis site to the nuclear pore before undergoing nucleocytoplasmic transport. Blobel [5] originally proposed localized vectorial transport of mRNAs from the nucleus (gene gating). Because the concentration of macromolecules in the nucleus is predicted to be high, one might expect a viscous intranuclear environment in which large RNPs would diffuse slowly (discussed in [6–8]). Contrary to this assumption, however, fluorescent RNAs microinjected into nuclei of living mammalian cells have been observed to localize at widespread nuclear sites [9–11], suggesting that RNAs might diffuse freely throughout the nucleus. Furthermore, recent measurements of the movement of molecules in the nucleus using fluorescence recovery after photobleaching and fluorescence correlation spectroscopy have suggested that dextrans, oligonucleotides and even large RNP complexes can move in the nucleus at rates close to those observed in aqueous solution [12,13]. These biophysical studies could not, however, visualize the movement of RNA within the spatial context of the nucleus. Such visualization is essential for understanding how RNAs are distributed within the nucleus of the live cell. Real-time tracking of endogenous RNA movement would allow analysis of the intranuclear disposition of the moving RNA over time as well as measurement of long-range diffusion coefficients. Using new labeling techniques and an imaging system that allows very rapid image acquisition, we have followed the movement of endogenous poly(A) RNA in the nuclei of living cells.

Results

Given that fluorescently labeled oligo(dT) hybridizes to intranuclear poly(A) RNA in live cells [13–15], we reasoned that it might be used as a tag to visualize and track poly(A) RNA movement *in vivo*. It is not straightforward, however, to distinguish between hybridized and free fluorescent

Figure 1

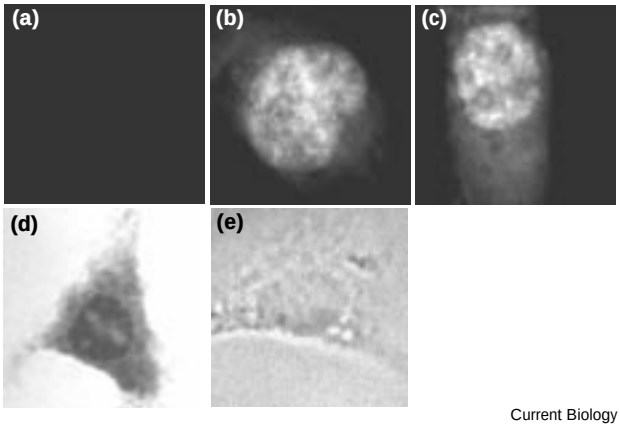

Caged fluorochrome-labeled oligo(dT) hybridizes to poly(A) RNA *in situ* and *in vivo*. (a–c) Caged FL–oligo(dT) or noncaged FL–oligo(dT) was hybridized to formaldehyde-fixed rat myoblasts *in situ* and signal was detected using a fluorescein filter set [18]. (a) The background signal from caged FL–oligo(dT) before uncaging. (b) An increase in fluorescence representing uncaged FL–oligo(dT) is observed in the nucleus after exposure to ultraviolet (UV) light through a DAPI filter set. (c) Noncaged FL–oligo(dT) hybridized to a myoblast *in situ*. (d,e) Live cells containing caged RG–oligo(dT) or RG–oligo(dA) were fixed and subjected to *in situ* reverse transcription [14,15] in which only hybridized oligonucleotide primes reverse transcription and incorporation of digoxigenin-labeled dUTP. Sites of digoxigenin incorporation, and therefore oligonucleotide hybridization, are visualized as a dark colored reaction product. (d) Cells containing caged RG–oligo(dT). (e) Cells containing caged RG–oligo(dA). All panels show contrast-enhanced digital images.

probe when observing live cells. By using a 'caged' probe in the present study, in which a protecting group prevents fluorescence until photolytic unmasking [16,17], only a small portion of the probe becomes fluorescent after spot photolysis of a small, spatially defined region of the nucleus, and the non-hybridized fraction of these small oligonucleotides rapidly diffuses to extinction in the large cellular volume. The hybridized probe, associated with larger poly(A) RNA molecules, can then be detected in the nucleus of live cells by the remaining fluorescent signal, and its spatial distribution and rate of movement analyzed.

Because rapid photoactivation is important when using caged molecules to track fast events, the uncaging rate of oligo(dT) labeled with various caged fluorochromes was measured in solution as described in Materials and methods. Oligonucleotides labeled with the caged fluorescein, CMNB2AF, were uncaged completely by the first time point assayed (about 30 seconds after uncaging), evidenced by the fact that the fluorescent intensity of the uncaged fluorescein remained essentially constant for 5 minutes (data not shown). Caged rhodamine green (RG) uncaged more slowly but was brighter and so was used for some qualitative experiments.

To confirm that the caged fluorescein-labeled oligo(dT) — termed caged FL–oligo(dT) — hybridized as expected to target poly(A) RNA, caged FL–oligo(dT) was first hybridized to fixed cells *in situ* using standard techniques [18]. The pattern of hybridization was similar to that seen using an oligo(dT) probe labeled with unmodified fluorescein (Figure 1a–c), indicating that the caged oligo(dT) probe hybridized to poly(A) RNA. Cells treated with caged oligo(dA) gave only background signal (data not shown). To test whether the caged oligo(dT) could also hybridize to poly(A) RNA in live cells, cells were incubated with caged oligo(dT) or control caged oligo(dA) under conditions known to allow *in vivo* hybridization of non-caged FL–oligo(dT) [13–15]. After a 1–2 hour efflux period, cells were fixed and used for reverse-transcriptase-mediated incorporation of digoxigenin-labeled dUTP to detect the sites of oligo(dT) hybridization [14–15]. Signal was observed only in cells treated with oligo(dT) and not in cells treated with oligo(dA), confirming that the modified oligo(dT) molecules had hybridized to poly(A) RNA effectively in live cells (Figure 1d,e).

To track the movement of the hybridized probe in the nucleus, live cells containing caged FL–oligo(dT) or caged FL–oligo(dA) were visualized using an inverted microscope interfaced with laser light sources and a digital imaging system capable of high-speed image acquisition (see Materials and methods). An approximately 2 μm diameter spot in the nucleus was irradiated using a 360 nm laser line directed through a pinhole and the distribution of the resulting fluorescent signal was recorded with time (Figure 2a). Fluorescence was observed at the uncaging site immediately (150 msec) after the laser pulse and then was seen to spread throughout the nucleus in all directions, excluding nucleoli, over the next 30 seconds. The intensity and distribution of the uncaged signal could be quantitatively analyzed in a highly sensitive way because the exact distribution of autofluorescent signal in the cell of interest is recorded in the caged image and can then be subtracted from the uncaged images on a pixel-by-pixel basis. About 10% of the oligo(dT) signal left the uncaging site by 1 second, and this number increased to approximately 45% at 10 seconds and 65% by 25 seconds, leaving one third of the signal at the uncaging site (Figure 2b). In contrast, over half of the uncaged control oligo(dA) had already diffused away by 1 second and over 90% had left the uncaging site by 10 seconds (Figure 2). These results were consistent with the hypothesis that the signal moving more slowly from the uncaged site in the oligo(dT) experiments represented oligo(dT)–poly(A) RNA hybrids.

To estimate the rate of oligo(dT) movement in the nucleus, the radial distance that signal traveled from the uncaging site (displacement) was measured in the seconds after uncaging (see Materials and methods). The mean square of the displacement varied linearly with time

Figure 2

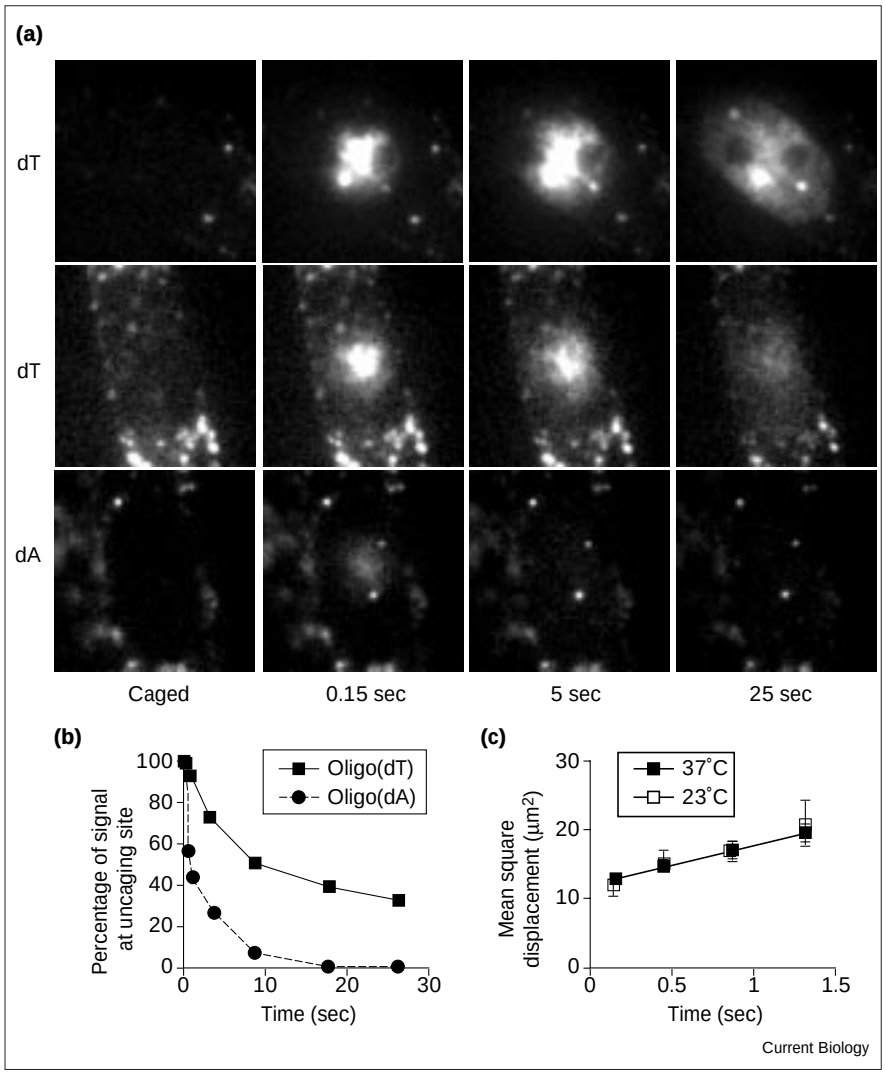

Movement of uncaged FL–oligo(dT) and FL–oligo(dA) in live rat cell nuclei. Caged fluorescein-labeled oligonucleotides taken up by myoblasts in culture were photolysed in a 2 μm intranuclear spot and successive images captured over time. (a) Two-dimensional images showing signal movement over time in both oligo(dT)- and oligo(dA)-containing nuclei. Autofluorescent perinuclear bodies are seen in the caged images. The nucleus in the top row contains high levels of uncaged oligo(dT) and is scaled differently than the nuclei in the middle and bottom rows. (Nuclei are ~10 μm in diameter; each image is ~19 μm × 19 μm.) (b) The amount of signal remaining at the uncaging site over time in nuclei containing oligo(dT) and oligo(dA). (c) The mean square displacement of the oligo(dT) signal (from the uncaging spot) at 37°C and 23°C plotted versus time. We estimate that, in an average nucleus, over 90% of the signal at the uncaging site represents hybridized oligo(dT), based on the assumption that unhybridized oligo(dT) is present at intranuclear levels similar to control unhybridized oligo(dA) or oligo(dN). See Materials and methods for details.

(R^2 = 0.985, Figure 2c) — a characteristic feature of diffusion [19]. We calculated an apparent diffusion coefficient of 0.6 ± 0.1 μm^2/sec. To further test the finding that the poly(A) RNA was diffusing, we performed the same experiments at 23°C instead of 37°C. Energy-requiring transport would be expected to slow considerably at the lower temperature, whereas diffusion would not (between the narrow range of 296–310°K). The spatial distribution of the uncaged signal was similar at the two temperatures and, as observed at 37°C, the oligo(dT) moved away from the site more slowly than control oligo(dA) (or than control oligo(dN), a mix of random sequence oligonucleotides; data not shown). Most significantly, the plot of the mean square displacements versus time at 23°C overlapped with the plot obtained from the 37°C data (P = 0.05, Figure 2c), indicating no differences between the apparent diffusion coefficients and demonstrating that an active transport process was unlikely. Hence, we conclude that diffusion is the most probable explanation for the movement of the poly(A) RNA.

It is worth noting that the amount of oligo(dT) remaining at the uncaging site, and in the nucleus as a whole, after 30 seconds was higher at 23°C than at 37°C (~60% compared with ~33%, Figure 2b and data not shown), as would be expected if poly(A)RNA export was reduced because of the lower activity of the (energy-dependent) nucleocytoplasmic transport process.

To examine the spatial distribution of poly(A) RNA throughout the nucleus at higher resolution, cells containing oligo(dT) were subjected to spot photolysis as described above and successive three-dimensional optical stacks were captured over time using high speed digital

Figure 3

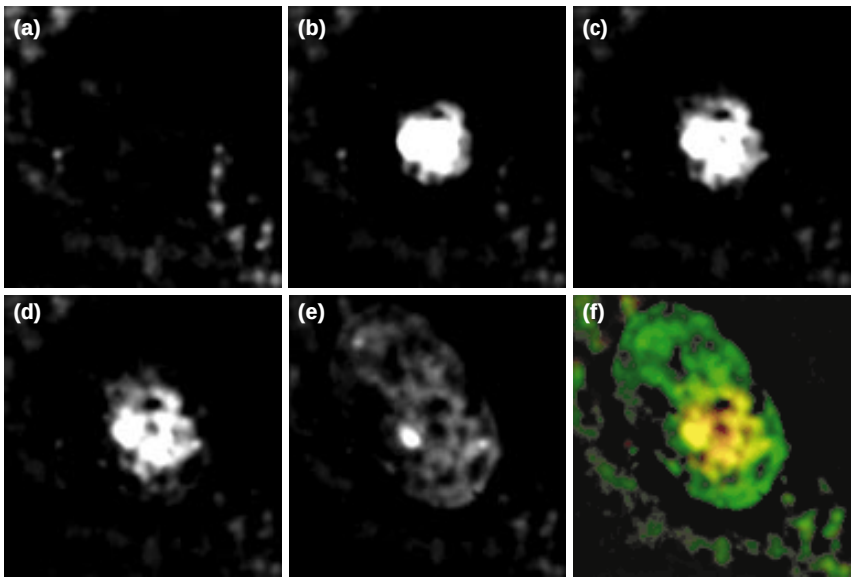

High resolution restoration of uncaged FL–oligo(dT) signal from three-dimensional image analysis. Cells containing caged FL–oligo(dT) were spot photolysed and multiple three-dimensional stacks, each containing 31 optical sections spaced 0.25 μm apart, were acquired over time. Out-of-focus light was restored to its proper spatial location using an iteration deconvolution algorithm (see Materials and methods), and identically scaled midsections from the (a) caged and (b–e) uncaged nucleus are shown at (b) 0.15 sec, (c) 1 sec, (d) 10 sec and (e) 150 sec after uncaging. (f) A qualitative comparison of the signal distribution of (d), in red, overlaid on (e), in green. The yellow colour indicates overlap. Each image is ~19 μm × 19 μm.

imaging (see Materials and methods). The increased resolution revealed that the poly(A) RNA hybridized to the uncaged oligo(dT) was confined to finger-like projections as it moved away from the uncaging site, with a somewhat lobular-like substructure (Figure 3). The width of the projections ranged from roughly 0.15–1.5 μm, and after spreading throughout the nucleus they assumed a more interconnected reticulate appearance. In restored images of nuclei containing both uncaged FL–oligo(dT) and Hoechst dye to stain DNA, the regions most intensely labeled by oligo(dT) were those least labeled by Hoechst and vice versa (Figure 4). Therefore, the poly(A) RNA was able to move throughout the interchromatin space in the nucleus.

Discussion

These results indicate that intranuclear trafficking of RNA can result from the simple, random process of diffusion throughout the interchromatin space. This conclusion is consistent with observations in other systems. In *Drosophila* polytene nuclei, pre-mRNA was deduced, from work *in situ*, to diffuse within 'channels' in the nucleus [6] and, in experiments *in vivo*, chromatin domains themselves were found to undergo constrained diffusion [8], supporting the idea of a nuclear environment conducive to diffusion. Fluorescence correlation spectroscopy (FCS) has also been used to measure the diffusion coefficients of oligo(dT)–poly(A) RNA hybrids in femtoliter regions within nuclei of living cells and in solution [13]. In these small intranuclear volumes, over half of the intranuclear oligo(dT)–poly(A) RNA hybrids moved at 'solution' rates, with an apparent diffusion coefficient of about 9 μm^2/sec. Because the small assay volume in the FCS measurements would often fit within the interchromatin channels observed here, and because the FCS sampling rate was very fast, it is likely that this number is a short-range estimate of the small scale diffusion of poly(A) RNA within a channel [20,21]. The apparent diffusion coefficient of 0.6 μm^2/sec estimated here was measured over relatively large distances (~5 μm) at a slower sampling rate, and therefore more accurately represents a value for long-range poly(A) RNA diffusion in the nucleus. The difference also fits well with the additional finding that the poly(A) RNA is confined to interchromatin channels, which would slow down poly(A) RNA movement over long distances and give rise to a lower apparent diffusion coefficient [20–22].

The slow population of poly(A) RNA that remained at the uncaging site after 30 seconds might represent molecules tethered to large macromolecular complexes, consistent with recent findings that showed that these complexes contain transcriptional, processing and polyadenylation machinery bound to DNA [23,24]. A portion of the poly(A) RNA population could also be diffusing within very small channels or microdomains and therefore not leave the site within the assay period.

The nuclear distribution pattern of poly(A) RNA observed in this study indicates that this RNA population can access virtually all of the non-chromosomal space in the nucleus, regardless of the uncaging location. This result is most consistent with a model which supposes that newly synthesized polyadenylated polymerase II transcripts diffuse randomly within the interchromatin space until they contact nuclear

Figure 4

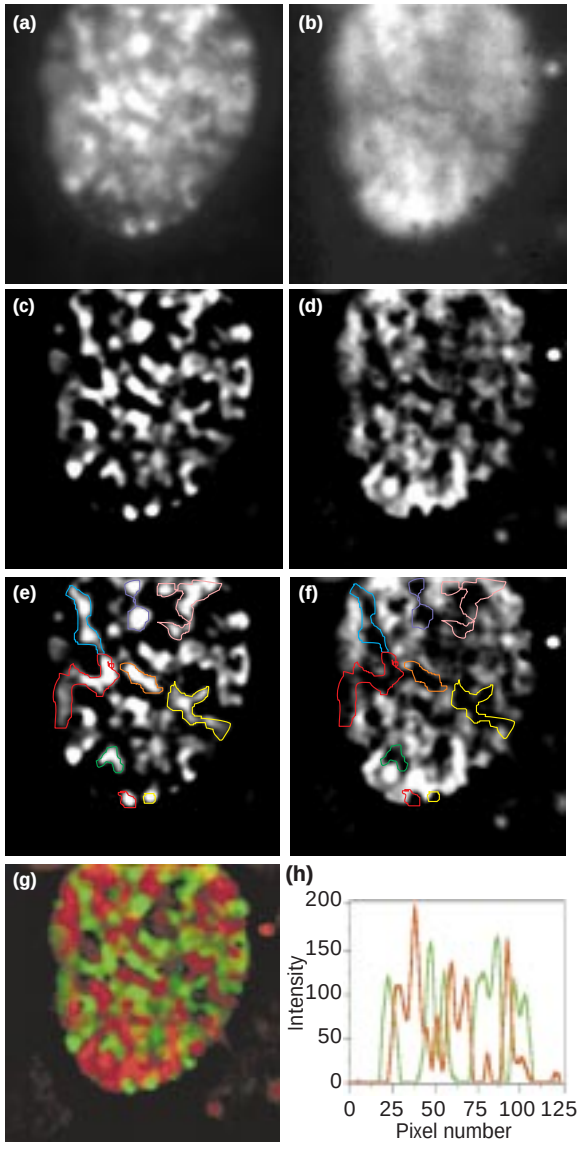

Intranuclear localization of uncaged FL–oligo(dT) compared to chromatin distribution. Cells were incubated sequentially with caged FL–oligo(dT) and Hoechst 33342 and three-dimensional stacks in both (**a**,**c**,**e**) blue (Hoechst-labeled chromatin), and (**b**,**d**,**f**) green (uncaged FL–oligo(dT), channels were captured and restored as described in Materials and methods. (a,b) Raw and (c,d) restored midsections show the distribution of Hoechst signal and uncaged FL–oligo(dT) signal in the same nucleus. (e,f) The same images as in (c,d) but high intensity regions of Hoechst signal were (e) outlined and (f) the outlines superimposed on the oligo(dT) image. (**g**) A color encoded overlay in which the Hoechst signal is green and the oligo(dT) signal is red. (**h**) A plot (linescan) of the intensity (arbitrary units) versus pixel number for the Hoechst (green) and oligo(dT) (red) signals as they vary along a line across the middle of (g). For (a–g), each image is ~19 μm × 19 μm.

pore components, a process which, according to our results, could occur in 30 seconds or less. We should point out that our results do not require invoking the existence of an ordered structure within the interchromatin space [24,25] but also do not rule it out. The results further imply that the freely diffusing RNA can access most, if not all, nuclear pores, which in the simplest case would predict a spherical distribution of export. It therefore appears unlikely that energy-requiring transport mechanisms with inherent directionality, such as those observed for the motor protein transport of organelles in the cytoplasm or of chromosomes during mitosis, operate within the nucleoplasm to move poly(A) RNA. This report marks the first step in a new approach to visualizing the spatial and temporal relationships between gene expression and nuclear structure.

Conclusions

Newly transcribed RNA must move from its site of synthesis to the nuclear pores so that transport into the cytoplasm can take place. We have found that endogenous poly(A) RNA can move freely about in the non-chromosomal space of the nucleus with properties characteristic of diffusion. These results suggest that mRNA may reach nuclear pores by the simple process of diffusion rather than by an energy-requiring process.

Materials and methods

Oligonucleotide synthesis, labeling and fluorimetry

Oligodeoxynucleotides (43mers, oligo(dT) or oligo(dA)) were automatically synthesized with an amino-modified thymidine at positions 2, 12, 22, 32 and 42. (Although the oligo(dA) contained thymidines at these positions, it is named oligo(dA) for simplicity.) Oligo(dN) contained a randomized population of 43mers theoretically containing 4^{38} different sequences, with amino-modified thymidines located as for oligo(dT) and oligo(dA). Oligonucleotides were gel purified, allowed to react with the N-hydroxylsuccinimidyl esters of the caged carboxyfluorescein, CMNB2AF, (a generous gift of Tim Mitchison, see also [16]) or caged rhodamine green (Molecular Probes) and labeled oligonucleotide was separated from unreacted dye using a Sephadex G-50 column [15]. For fluorimetry, solutions containing oligo(dT) labeled with caged fluorochromes (10 ng/μl in water) were irradiated in a cuvette placed in the path of a 360 nm laser beam (~30 W/cm^2) for 100 msec. The intensity of the uncaging fluorescein oligonucleotides was then monitored over time in a Spex Fluorolog 2 fluorimeter (excitation 492 nm, emission 515 nm).

Cell culture and oligonucleotide uptake

Rat L6 myoblasts growing in Dulbecco's Modified Eagle's Medium on 25 mm round coverslips were allowed to take up oligonucleotides alone [14] or oligonucleotides complexed with the cationic lipids, Tfx-50 (Promega) or Pfx-6 (Invitrogen) [15]. Oligonucleotide was either added directly with culture medium (without serum) at a final concentration of 1 μM or mixed with cationic lipid to give a final oligonucleotide concentration of 0.10–0.25 μM. Cells were incubated with oligonucleotide (with or without cationic lipid) for 2 h, rinsed, and unbound oligonucleotide allowed to efflux for at least 1 h in serum-containing medium. These conditions gave maximal levels of oligo(dT) hybridization to poly(A) RNA, as evaluated using *in situ* reverse transcription [14,15]. In some experiments, Hoechst dye 33342 (Molecular Probes) was added to the medium during the efflux period (final concentration, 2.5 μM).

Microscopy, laser photoactivation, image acquisition and analysis

The imaging workstation consisted of a custom-built inverted microscope, equipped with both visible and UV lasers and a piezoelectric

focus translator for high-speed three-dimensional optical sectioning, interfaced with a high speed, low noise CCD camera (128 × 128 pixel format; MIT Lincoln Laboratory) and a Pentium PC with high-speed image acquisition boards (see also [26,27]). Labeled oligonucleotide in the nuclei of live myoblasts (growing on a coverslip at 37°C in Leibowitz L-15 medium (Gibco) with 10% serum) was typically uncaged for 65 msec in a 2 μm diameter spot by passing 360 nm light, isolated from a multiline argon laser, through a small (100 or 60 μm) pinhole before direction through a 40× oil (UV-transmissible fluor) or 100× glycerine (UV-F) objective (both 1.3 NA, Nikon) onto the cell. Uncaged fluorescence was then excited using the 488 nm line of an argon laser and the emission detected using a 500 nm long pass cut-off filter. In some experiments, Hoechst dye was also excited at 360 nm. A single dichroic mirror (Chroma 505DCLPXR) that allowed extended reflection for UV light was used. Cells were exposed to ~1.6 kW/cm^2 of 360 nm light at the uncaging site (~0.1–0.5 kW/cm^2 for Hoechst detection) and 0.01–0.1 kW/cm^2 of 488 nm light to excite the uncaged fluorochrome. Cells appeared to grow normally for at least 24 h after microscopic observation.

For quantitation, two-dimensional images of each uncaged nucleus were captured every 450 msec over 30 sec. The intensity array of autofluorescence present in a given caged image was then subtracted on a pixel-by-pixel basis from each subsequent uncaged image using standard imaging software (that is, from Metamorph, Universal Imaging Corp). This method of background subtraction allows the removal of the actual autofluorescence signal at each pixel and differs from standard techniques of background subtraction where an average background value is estimated and subtracted from all pixels. The average intensity at the uncaging site (defined as a ~4 μm^2 box) at each time was then measured and corrected for bleaching using the bleach rate observed with (noncaged) FL–oligo(dT) under identical conditions (~20% at the end of this acquisition protocol). Three-dimensional stacks consisted of 31 optical sections, spaced 0.25 μm apart, captured at a 10 msec exposure time per section for fluorescein and 2 msec per section for Hoechst detection. (This minimal UV exposure time for Hoechst-labeled cells was critical to their survival.) Three-dimensional image stacks were then subjected to exhaustive photon reassignment to return out-of-focus light to its correct location (pixel size, 150 nm; smoothness factor, 2×10^{-3}; iterations, 120; convergence, 10^{-3} [28]).

Calculation of radial movement of signal (ω^2)

The laser intensity at the uncaging site describes a Gaussian distribution, which for a single Gaussian takes the form of $A = A_0 e^{-2r^2/\omega^2}$, where A_0 = maximum intensity and A = intensity at radius, r. The solution of the diffusion equation for a Gaussian initial intensity is:

$$A(r,t) = \frac{A_0}{(1 + 8Dt/\omega^2)} e^{-2r^2/\omega^2 (1+8Dt/\omega^2)} \quad (1)$$

as discussed [29]. In our analysis, the mean square displacement (ω^2) was calculated from two-dimensional images as the average of the squares of the signal distribution radius at Ae^{-2} where A = maximum intensity from each time point. The intensities and correct radii for each time point were determined from the average of at least five linescans across the uncaging site at various azimuth angles using Metamorph software (after subtraction of the caged image as described above). After plotting ω^2 versus t, the diffusion coefficient was estimated from the slope of the unweighted least-squares fit line using $\omega^2 = 8Dt$ [29].

Acknowledgements

We thank Tim Mitchison (Harvard Medical School) for the generous gift of a soluble caged carboxyfluorescein, David Wolf and Elizabeth Browne (University of Massachusetts Medical School) for many helpful discussions, Susan Kilroy (the Pederson lab) for expert technical help, Anka Ehrhardt (University of Massachusetts Medical School) for help with fluorimetry, and Douglas Bowman (Universal Imaging Systems), Lawrence Lifshitz, Mark Nadler, and Kevin Fogarty (University of Massachusetts Medical School) for help with digital imaging analysis. This research was supported by NIH NRSA postdoctoral fellowship AR-08361 to J.C.P., NIH grant GM-21595-22 to T.P., NIH grant GM-54887 to R.H.S. and NSF grants DBI9200027 and DBI9724611 to the Biomedical Imaging Facility at the University of Massachusetts Medical School. This work was facilitated at its outset by our late colleague Fredric S. Fay, who gave us support and encouragement. We dedicate this paper to his memory.

References

1. Stutz F, Rosbash M: Nuclear RNA export. *Genes Dev* 1998, 12:3303-3319.
2. Dahlberg JE, Lund E: Functions of the GTPase Ran in RNA export from the nucleus. *Curr Opin Cell Biol* 1998, 10:400-408.
3. Mattaj IW, Englmeier L: Nucleocytoplasmic transport: the soluble phase. *Annu Rev Biochem* 1998, 67:265-306.
4. Englmeier L, Olivo JC, Mattaj IW: Receptor-mediated substrate translocation through the nuclear pore complex without nucleotide triphosphate hydrolysis. *Curr Biol* 1999, 9:30-41.
5. Blobel G: Gene gating: a hypothesis. *Proc Natl Acad Sci USA* 1985, 82:8527-8529.
6. Zachar Z, Kramer J, Mims IP, Bingham PM: Evidence for channeled diffusion of pre-mRNAs during nuclear RNA transport in metazoans. *J Cell Biol* 1993, 121:729-742.
7. Agutter PS: Models for solid-state transport: messenger RNA movement from nucleus to cytoplasm. *Cell Biol Int* 1994, 18:849-858.
8. Marshall WF, Straight A, Marko JF, Swedlow J, Dernburg A, Belmont A, *et al.*: Interphase chromosomes undergo constrained diffusional motion in living cells. *Curr Biol* 1997, 7:930-939.
9. Wang J, Cao LG, Wang YL, Pederson T: Localization of pre-messenger RNA at discrete nuclear sites. *Proc Natl Acad Sci USA* 1991, 88:7391-7395.
10. Jacobson MR, Cao LG, Wang YL, Pederson T: Dynamic localization of RNase MRP RNA in the nucleolus observed by fluorescent RNA cytochemistry in living cells. *J Cell Biol* 1995, 131:1649-1658.
11. Jacobson MR, Cao LG, Taneja KL, Singer RH, Wang YL, Pederson T: Nuclear domains of the RNA subunit of RNase P RNA. *J Cell Sci* 1997, 110:829-837.
12. Seksek O, Biwersi J, Verkman AS: Translational diffusion of macromolecule-sized solutes in cytoplasm and nucleus. *J Cell Biol* 1997, 138:131-142.
13. Politz JC, Browne ES, Wolf DE, Pederson T: Intranuclear diffusion and hybridization state of oligonucleotides measured by fluorescence correlation spectroscopy in living cells. *Proc Natl Acad Sci USA* 1998, 95:6043-6048.
14. Politz JC, Taneja KL, Singer RH: Characterization of hybridization between synthetic oligodeoxynucleotides and RNA in living cells. *Nucleic Acids Res* 1995, 23:4946-4953.
15. Politz JC, Singer RH: ***In situ*** reverse transcription for the detection of hybridization between oligonucleotides and their intracellular targets. *Methods* 1999, in press.
16. Mitchison TJ, Sawin KE, Theriot JA, Gee K, Mallavarapu A: Caged fluorescent probes. *Methods Enzymol* 1998, 291:63-78.
17. Mitchison TJ: Polewards microtubule flux in the mitotic spindle: evidence from photoactivation of fluorescence. *J Cell Biol* 1989, 109:637-652.
18. Taneja KL, Lifshitz LM, Fay FS, Singer RH: Poly(A) RNA codistribution with microfilaments: evaluation by ***in situ*** hybridization and quantitative digital imaging microscopy. *J Cell Biol* 1992, 119:1245-1260.
19. Einstein A: *Investigations on the Theory of Brownian Movement.* New York: Dover Publishing; 1956.
20. Saxton MJ: Single-particle tracking: effects of corrals. *Biophys J* 1995, 69:389-398.
21. Saxton MJ: Single-particle tracking: the distribution of diffusion coefficients. *Biophys J* 1997, 72:1744-1753.
22. Olveczky BP, Verkman AS: Monte Carlo analysis of obstructed diffusion in three dimensions: application to molecular diffusion in organelles. *Biophys J* 1998, 74:2722-2730.
23. Steinmetz EJ: Pre-mRNA processing and the CTD of RNA polymerase II: the tail that wags the dog? *Cell* 1997, 89:491-494.
24. Misteli T, Spector DL: The cellular organization of gene expression. *Curr Opin Cell Biol* 1998, 10:323-331.
25. Pederson T: Thinking about a nuclear matrix. *J Mol Biol* 1998, 277:147-159.

26. Rizzuto R, Pinton P, Carrington W, Fay FS, Fogarty KE, Lifshitz LM, *et al.*: Close contacts with the endoplasmic reticulum as determinants of mitochondrial Ca^{2+} responses. *Science* 1998, 280:1763-1766.
27. Rizzuto R, Carrington W, Tuft RA: Digital imaging microscopy of living cells. *Trends Cell Biol* 1998, 8:288-292.
28. Carrington WA, Lynch RM, Moore ED, Isenberg G, Forgarty KE, Fay FS: Superresolution three-dimensional images of fluorescence in cells with minimal light exposure. *Science* 1995, 268:1483-1487.
29. Cardullo RA, Mungovan RM, Wolf DE: Imaging membrane organization and dynamics. In *Biophysical and Biochemical Aspects of Fluorescence Spectroscopy.* Edited by Dewey TD. New York: Plenum Publishing; 1991:231-260.

Because *Current Biology* operates a 'Continuous Publication System' for Research Papers, this paper has been published on the internet before being printed. The paper can be accessed from http://biomednet.com/cbiology/cub – for further information, see the explanation on the contents page.